Synthesis of circularly-polarized parasitic micro-array using spherical wave expansion

Hussein Jaafar, Antonio Clemente, Christophe Delaveaud, Thierry Le Nadan

Synthesis of Circularly Polarised Parasitic Micro-Array Using Spherical Wave Expansion

Hussein Jaafar[1], Antonio Clemente[1], Christophe Delaveaud[1],Thierry le Nadan[2]
[1]CEA-LETI, MINATEC Campus, Université Grenoble-Alpes, 38400 Grenoble, France (hussein.jaafar@cea.fr)
[2]Radiall,38340 Voreppe, France (thierry.lenadan@radiall.com)

***Abstract*— This paper presents the design of a Right-Hand Circularly Polarized (RHCP) electrically small micro-array. The design principle is composed of a highly coupled three-IFA radiators distributed over a radial configuration. Only one antenna is driven, while optimized parasitic loads are connected on the non-driven elements. The parasitic load values are computed using the Spherical Wave Expansion (SWE) optimization, where an Circularly Polarized (CP) objective radiation is defined. The proposed antenna having an electrical size ka=0.6 exhibits an RHCP radiation in the GPS-L2 band with an 4dBic Gain.**

***Index Terms*—GPS, GNSS,SWE, Electrically Small Antenna (ESA).**

I. INTRODUCTION

Over the last decade, the wireless revolution have witnessed an exponential increase in the number of connected objects. This imposed a higher demand on the use of the Global Navigation Satellite Systems (GNSS) for a vast variety of applications, ranging from low-end mobile device navigation, up to high-end vehicle localization, geographical surveys, UAV as well as military applications. To fulfill the GNSS standard, the associated antenna must exhibit an RHCP radiation and a flat gain over the bandwidth of operation. Yet, the size of the antenna remains a critical issue for most GNSS systems where more compact, low profile, and low-cost modules are required [1], [2].

Typically, RHCP is realized by exciting two orthogonal degenerate modes, while insuring a desired 90° relative phase. Extensive RHCP antenna designs have been reported in literature. Most of the research works focus mainly on three antenna categories: ceramic patches, crossed dipoles and quadri-filiar helix antennas [3]–[5]. Other emerging designs such as metamaterial inspired circularly polarized antennas [6], and 3-element IFA structures [7] have recently been reported . Yet, the proposed configurations, do not simultaneously satisfy the antenna requirement in terms of size, cost and design complexity.

While the multi-element antenna design [7]–[8] presents a simple and compact solution, a feeding network is still required to achieve the desired relative phase shifts between the radiation elements. This will consequently increase the cost and the complexity of the design. In order to surpass this requirement, the authors in [9], proposed a parasitic dual band multi-element RHCP IFA-based micro-array. In this configuration, only one antenna is fed, while the others are terminated with parasitic loads. The parasitic load values are optimized based on a design automation tool. The tool uses the SWE in order to set the objective CP radiation, then searches for the appropriate load configuration that yields a radiation pattern having the highest correlation with the objective radiation.

This paper proposes the design of a 3-element IFA parasitic µ-array operating in the GPS-L2. Up to the authors' knowledge, such configuration have not yet been reported in literature. The optimized parasitic load values are calculated based on a SWE optimization approach. The design methodology is presented in Section II, followed by a demonstration of the CP 3-element parasitic IFA array in Section III. Finally, Section IV discusses the perspective for the design of a multiband parasitic configuration.

II. DESIGN METHODOLOGY

The design approach is inspired by the method presented in [10], where the authors utilized the SWE to maximize the directivity of a 4-element compact array. Form a SWE point of view, any radiated field can be expressed a linear combination of the far-field spherical wave pattern functions $\vec{K}_{smn}(\theta,\phi)$ as given in (1):

$$\vec{E}(r,\theta,\phi) = \sqrt{\eta}\frac{k}{\sqrt{4\pi}}\frac{e^{-jkr}}{kr}\sum_{smn} Q_{smn}.k_{smn}(\theta,\phi) \quad (1)$$

Where η is the impedance of the medium, Q_{smn} are the spherical wave coefficients, n is the degree limited by $|m| < n$, and $s = 1,2$ indicates the coefficient TE- and TM- wave respectively. For the case of a P element array, the total radiated field can be expressed as a weighted summation of the fields radiated by the active elements:

$$\vec{E}(\theta,\phi) = \sum_{p=1}^{P} \alpha_p \vec{E}_p(\theta,\phi) \quad (2)$$

Substituting (1) in (2) yields :

$$Q_{smn}^{total} = \sum_{p=1}^{P} \alpha_p Q_{smnp} \quad (3)$$

Hence in order to synthesize a desired radiation pattern, it is sufficient to solve α_p in (3), where Q_{smn}^{total} is substituted by an

objective radiation $Q_{smn}^{objective}$. In [10], $Q_{smn}^{objective}$ is set to the spherical wave coefficients that maximize the directivity of a linear array. Alternatively, in the proposed approach, the $Q_{smn}^{objective}$ is associated to a circularly polarized radiation which will be defined in the next section.

Once the weighting coefficients α_p are calculated, the associated parasitic loads are easily computed using the network model of the array [10].

III. 3-IFA PARASITIC μ-ARRAY

The geometry of the proposed micro-array is shown in Fig. 1. The array is composed of three IFAs distributed around a cylindrical circumference of radius R=22.5 mm. The array elements denoted by IFA_1,IFA_2, and IFA_3 are excited at the ports 1, 2 and 3 respectively. With the given dimensions, the electrical size of the micro-array is ka~0.6, implying an electrically small configuration. In order to surpass the complexity of the design process, the geometry of driven element IFA_1 with height h_1=26.35 mm is distinct from the other two parasitic identical antennas (IFA_2 and IFA_3 with height h_2=22.44 mm). This distinction is essential to introduce an additional degree of freedom in order to properly tune the array elements, especially for the case of such a tightly coupled configuration, where the radiation and impedance behavior of the elements are extremely sensitive.

Fig. 2 (a) examines the impact of placing the IFAs in the proposed highly coupled configuration. The influence is mainly visible for IFA_2 and IFA_3 where the matching frequency shifts from 1.3 GHz down to 1.2 GHz and 1.15 GHz for IFA_2 and IFA_3 respectively. On the other hand, the impact on the modified IFA_1 is limited compared to the other IFAs. This remarkable modification is due to the high intrinsic coupling between the micro-array elements (Fig. 2 (b)). In the vicinity of the GPS-L2 band, the coupling between IFA_2 and IFA_3 ($|S_{23}|$) attains a maximum value of -4 dB, while the coupling between IFA_1 and the parasitic elements is limited between -9 dB and -8dB.

After defining the array geometry, the active radiation patterns of the array elements at the central frequency 1.225 GHz are extracted. The spherical wave coefficients of each array element are then calculated based on (1). Finally, the optimized weighting coefficients α_p are computed based on the predefined objective function. In this study, two objective function are examined. The first objective function denoted by Q_{smn}^{obj1} corresponds to an ideal Circular Polarization, where two radiation modes with equal magnitudes and opposite phase are combined (Fig. 3). On the other hand, the second objective function Q_{smn}^{obj2}, presents a sub-optimal case, where the weights of the principle modes are modified and higher order modes are introduced (Fig. 4).

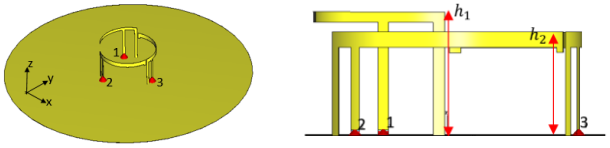

(a) (b)

Fig. 1. Geometry of the 3-IFA micro-array. (a) 3D View, (b) side view.

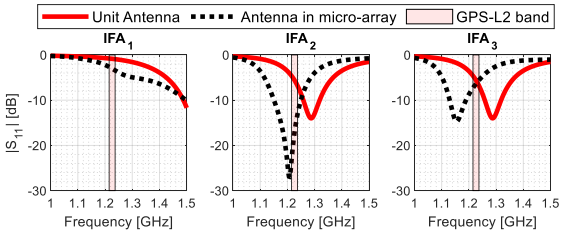

(a)

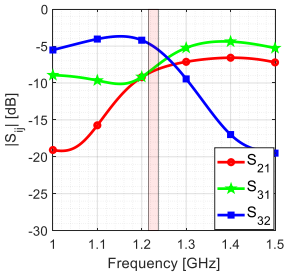

(b)

Fig. 2. Scattering parameters of the micro-array. (a) Input reflection coefficient of the isolated antennas compared to the micro-array elements, (b) intrinsic coupling of the micro array.

A. Objective function: Q_{smn}^{obj1}

Fig. 3 shows the radiation characteristics of the ideal objective function Q_{smn}^{obj1}. The CP radiation is achieved by combining the TE_{-11} and the TM_{-11} modes with equal magnitudes and a 180° phase shift. This combination yields a principle RHCP radiation pattern (curve in blue) while the LHCP is null. Resolving (3) based on Q_{smn}^{obj1}, yields the parasitic loads given in Table 1. With the given loading configuration the array exhibits an RHCP radiation with an AR<3dB in the targeted GPS-L2 band (Fig. 5). However, in order to achieve such performance, a negative resistive load (R=-2.75 Ohm) is required at port 3. While realizing a negative resistance is possible through Negative Impedance Convertors (NICs) [11], such step adds significant complexity to the design and fabrication process.

Two possible strategies could be adopted in order to eliminate the need for the negative resistance to achieve a CP radiation. The first approach is by applying geometrical modification on the IFAs. Hence, this induces variations in the coupling and the reflection coefficients of micro-array elements. These modifications will consequently alter the values of the optimized parasitic loads. However, such approach requires tedious parametric modifications and associated EM simulations, which might be time consuming. A more simple approach is to modify the objective function.

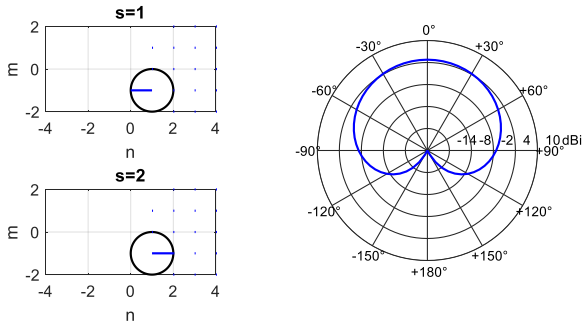

(a) (b)

Fig. 3. Ideal objective function. (a) Spherical wave coefficients, (b) radiation pattern.

Table 1 Optimized parasitic loads at 1.225 GHz based on Q_{smn}^{obj1}.

PORT	R [Ohm]	C [pF]
2	8.8	6.1
3	-2.75	3.7

This implies defining a sub-optimal objective radiation in order to relax the optimization equation. The advantage of such approach is that it does not require any geometrical modifications nor new EM simulations. All the results are obtained through simple post-processing.

B. Objective function: Q_{smn}^{obj2}

The modified objective function Q_{smn}^{obj2} is shown in Fig. 4. In addition to the dominant contribution of the principle radiating modes TE_{-11} and TM_{-11}, a slight contribution of the modes TE_{01}, and TM_{01} is introduced. The weighted contribution of the defined spherical modes is given in Table 2. The combination of the defined modes yields the radiation pattern of Fig. 4 (b), where the LHCP (red curve) appears, with however a negligible impact on the purity of the RHCP (blue curve).

Contrary to Q_{smn}^{obj1}, the optimized resistive parasitic loads associated to the modified "sub-optimal" objective function Q_{smn}^{obj2} exhibit very low values which could be neglected without impacting the desired radiation performance (Table 3). Therefore, the parasitic configuration contains purely capacitive loads where C_2=6.2 pF at port 2 and C_3=3 pF at port 3. Hence, with the given parasitic configuration, the array exhibits an RHCP radiation with a maximal gain of 4 dBic, AR~1dB and a 94% radiation efficiency at the central frequency 1.225 GHz (Fig. 5). The high radiation efficiency is directly correlated to the absence of resistive parasitic loads. Nevertheless, the LHCP levels increase at the extremity of the GPS-L2 band due to the sensitivity of the design towards the parasitic load values. This implies an increase in the AR levels which attains 5 dB at 1.237 GHz. This AR level could be further enhanced by fine tuning the parasitic load values.

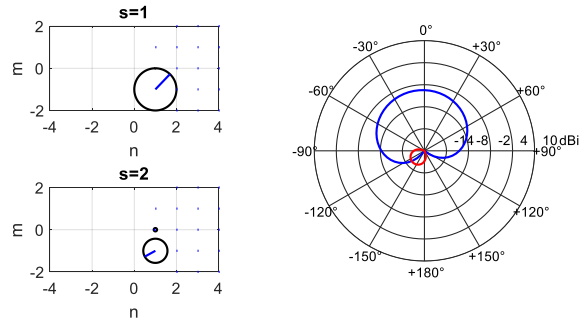

(a) (b)

Fig. 4. Modified objective function. (a) Spherical wave coefficients, (b) radiation pattern.

Table 2 Modal contribution of Q_{smn}^{obj2}.

Contributing Modes	Amplitude	Phase [°]
TE_{-11}	0.44	0
TM_{-11}	0.37	162
TE_{01}	0.01	273
TM_{01}	0.12	144

Table 3 Optimized parasitic loads at 1.225 GHz based on Q_{smn}^{obj1}

PORT	R [Ohm]	C [pF]
2	0.39→ 0	6.2
3	-0.24→ 0	3

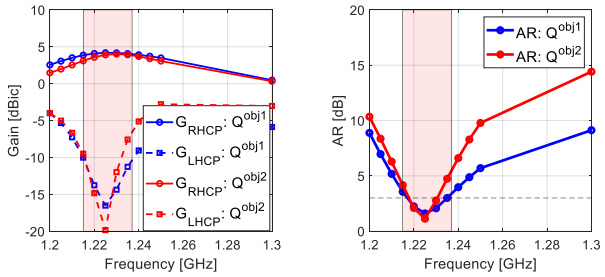

(a) (b)

Fig. 5. Radiation performance of the optimized parasitic arrays. (a) Intrinsic Gain in the boreside direction ($\theta = 0°, \phi = 0°$), (b) axial ratio.

IV. CONCLUSION

The design concept of an electrically small RHCP parasitic micro-array is proposed in this paper. The design optimization based on the SWE is introduced, shedding the light on the impact of the objective function on the values of the optimized parasitic loads. By using a sub-optimal objective function (Q_{smn}^{obj2}), it was possible to obtain purely reactive parasitic loads, implying less resistive losses. The simulated parasitic array demonstrates promising performance in terms of polarization purity and radiation efficiency. Future work will focus on the fabrication and measurement of the proposed structure, as well as extending the studies towards a multi-band configuration using co-localized micro-arrays.

REFERENCES

[1] Nasimuddin, X. Qing, et Z. N. Chen, "A Compact Circularly Polarized Slotted Patch Antenna for GNSS Applications", *IEEE Trans. Antennas Propag.*, vol. 62, nº 12, p. 6506-6509, Dec. 2014, doi: 10.1109/TAP.2014.2360218.

[2] E. Arnaud, L. Huitema, R. Chantalat, A. Bellion, et T. Monediere, "Miniaturization of a circular polarized antenna using ferrite materials", in *12th European Conference on Antennas and Propagation (EuCAP 2018)*, April. 2018, p. 1-5. doi: 10.1049/cp.2018.0917.

[3] Z. Wang, S. Fang, S. Fu, et S. Lu, "Dual-Band Probe-Fed Stacked Patch Antenna for GNSS Applications", *IEEE Antennas Wirel. Propag. Lett.*, vol. 8, p. 100-103, 2009, doi: 10.1109/LAWP.2008.2012355.

[4] S. X. Ta, H. Choo, I. Park, et R. W. Ziolkowski, "Multi-Band, Wide-Beam, Circularly Polarized, Crossed, Asymmetrically Barbed Dipole Antennas for GPS Applications", *IEEE Trans. Antennas Propag.*, vol. 61, nº 11, p. 5771-5775, Nov. 2013, doi: 10.1109/TAP.2013.2277915.

[5] J. Lei, G. Fu, et Y. Hao, "Wideband printed tapering quadrifilar helical antenna for GNSS", in *2015 9th European Conference on Antennas and Propagation (EuCAP)*, April. 2015, p. 1-2.

[6] L. Garcia-Gamez *et al.*, " Compact GNSS Metasurface-Inspired Cavity Antennas", *IEEE Antennas Wirel. Propag. Lett.*, vol. 18, nº 12, p. 2652-2656, Dec. 2019, doi: 10.1109/LAWP.2019.2947791.

[7] L. H. Trinh, N. V. Truong, et F. Ferrero, "Low Cost Circularly Polarized Antenna for IoT Space Applications", *Electronics*, vol. 9, nº 10, Art. nº 10, Oct. 2020, doi: 10.3390/electronics9101564.

[8] W.-I. Son, W.-G. Lim, M.-Q. Lee, S.-B. Min, et J.-W. Yu, "Design of Compact Quadruple Inverted-F Antenna With Circular Polarization for GPS Receiver", *IEEE Trans. Antennas Propag.*, vol. 58, nº 5, p. 1503-1510, May 2010, doi: 10.1109/TAP.2010.2044344.

[9] L. Rudant, L. Batel, A. Clemente, et C. Delaveaud, " New Approach in Antenna Design Automation Applied to a Dual-Band GNSS Micro-Array", in *2021 15th European Conference on Antennas and Propagation (EuCAP)*, Dusseldorf, Germany, Mar. 2021, p. 1-5. doi: 10.23919/EuCAP51087.2021.9411019.

[10] A. Clemente, M. Pigeon, L. Rudant, et C. Delaveaud, " Design of a Super Directive Four-Element Compact Antenna Array Using Spherical Wave Expansion", *IEEE Trans. Antennas Propag.*, vol. 63, nº 11, p. 4715-4722, Nov. 2015, doi: 10.1109/TAP.2015.2475617.

[11] J. G. Linvill, " Transistor Negative-Impedance Converters", *Proc. IRE*, vol. 41, nº 6, p. 725-729, June 1953, doi: 10.1109/JRPROC.1953.274251.